

Lecture 8

- Double-diffusive convection
- Discovered in oceanographic context
- Nowadays many applications
- Here: two diffusivities
- Thermal diffusivity acts *destabilizing*
- In astrophysics: semiconvection

Different diffusivities crucial

- $\kappa_S = 1.3 \times 10^{-5} \text{ cm}^2 \text{ s}^{-1}$ (sea water)
- $\kappa_C = 1.5 \times 10^{-3} \text{ cm}^2 \text{ s}^{-1}$
- $\text{Le} = \kappa_T / \kappa_C = \text{Sc} / \text{Pr} = \text{Schmidt} / \text{Prandtl}$
 - is large
 - temperature in equilibrium, salinity not
- Diffusion can destabilize the system!
 - not with single diffusing component

Two active scalars

$$\rho = \rho_{00} [1 - \alpha_T (T - T_{00}) + \alpha_C (C - C_{00})]$$

- C for concentration of salinity
 - avoid S , which we used for entropy
 - both $\alpha_T > 0$ and $\alpha_C > 0$
 - Opposing trends:
 - if T increases, ρ decreases
 - if C increases, ρ increases
- Rayleigh-Benard-like problem

The “Salt-Fountain” and Thermohaline Convection

By MELVIN E. STERN, Woods Hole Oceanographic Institution

(Manuscript received January 4, 1960)

Abstract

A “gravitationally stable” stratification of salinity and temperature, such as is observed in the oceans, is actually unstable due to the fact that the *molecular* diffusivity of heat is much greater than the diffusivity of salt. We discuss this stability characteristic and the form of the convective motion in the laminar regime. Future studies of this model relative to the amplitude of the motion and the subsequent transition to turbulence should lead to the formulation of critical observational questions, which will determine whether the proposed mechanism is significant in the vertical mixing of the sea.

STOMMEL, ARONS and BLANCHARD (1956) have described an “oceanographical curiosity” by noting that if a long vertical tube was lowered into the ocean, in such a manner that its bottom was exposed to cold fresh water and its top to warm saline water, a continuous motion could be maintained therein after priming the fountain. Their explanation is that the ascending (or descending) water in the tube would exchange heat but not salinity with the ambient ocean and would be accelerated due to its deficit in salt and density relative to fluid at the same level outside the tube. The purpose of this note, stemming

free convection, despite the fact that the mean density field increases in the direction of gravity. The decrease of mean salinity in this direction provides the energy source for the convective motions, and if this salt gradient is maintained by climatological factors then it furnishes a mechanism, whose relative importance must be determined, for the vertical transport of salt and heat in the ocean.

In order to forestall premature discussion of eddy exchange coefficients let us first consider an isolated system consisting of a horizontal convection chamber whose top surface is maintained at a higher temperature and salinity than the

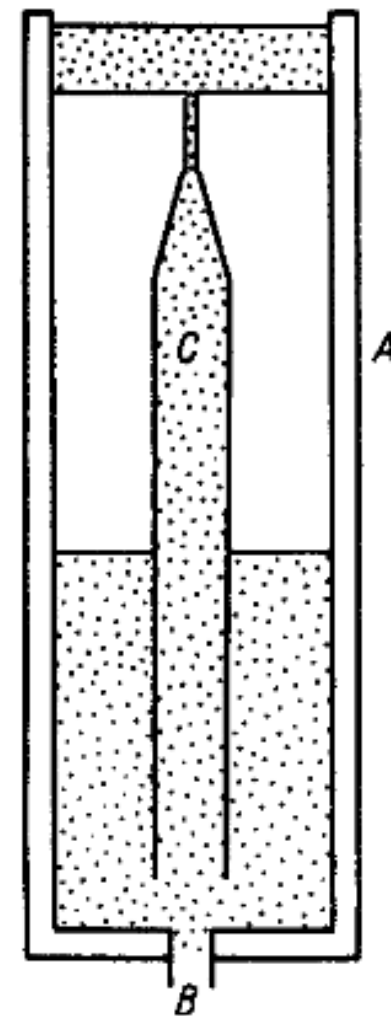

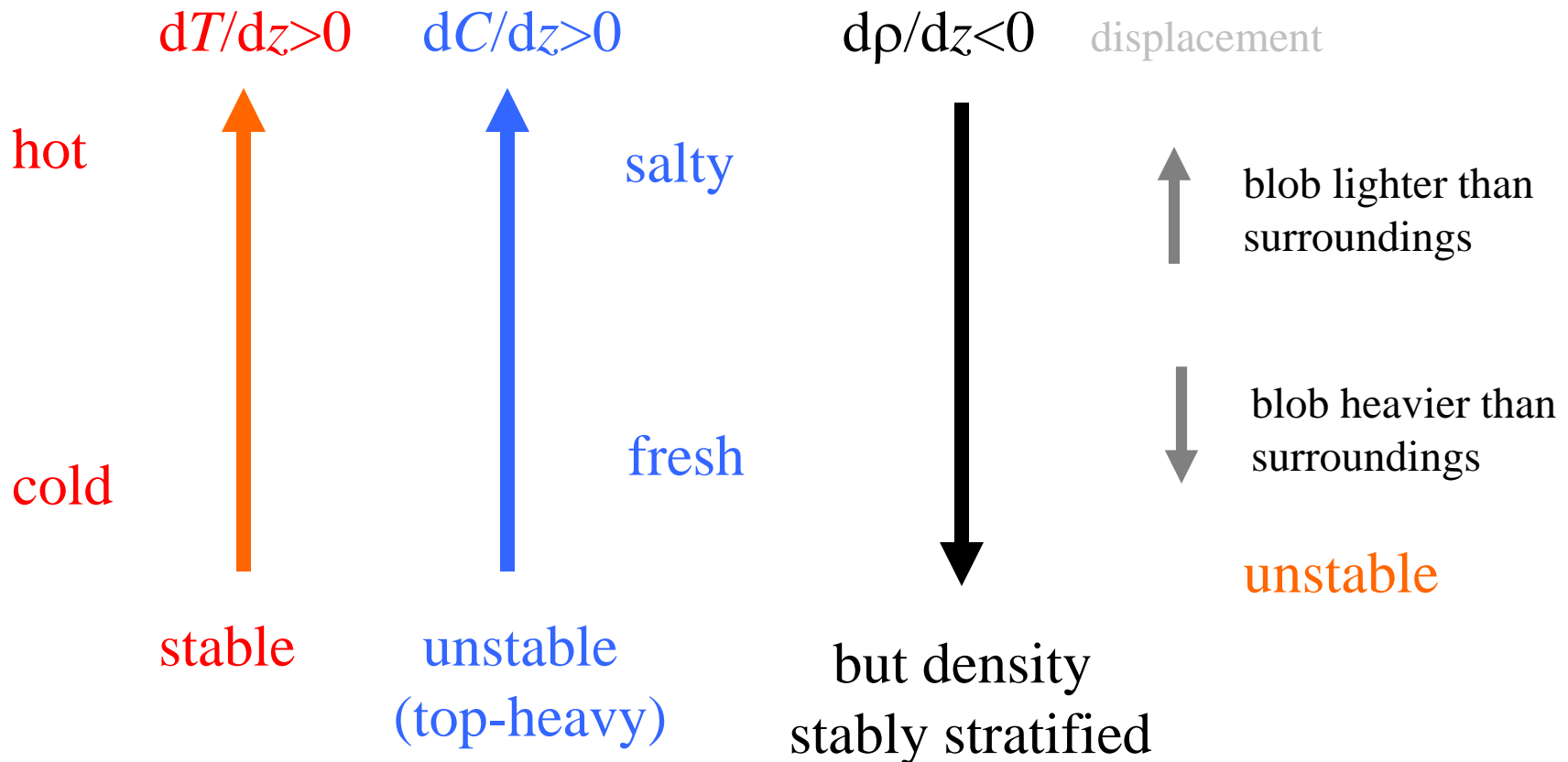


Fig. 1. Laboratory experiment to demonstrate the salt fountain, showing outside glass tube A, with hole in the bottom for filling B, and inner glass tube C to produce the fountain. The shading indicates the coloured water after the fountain has been in operation for some time.

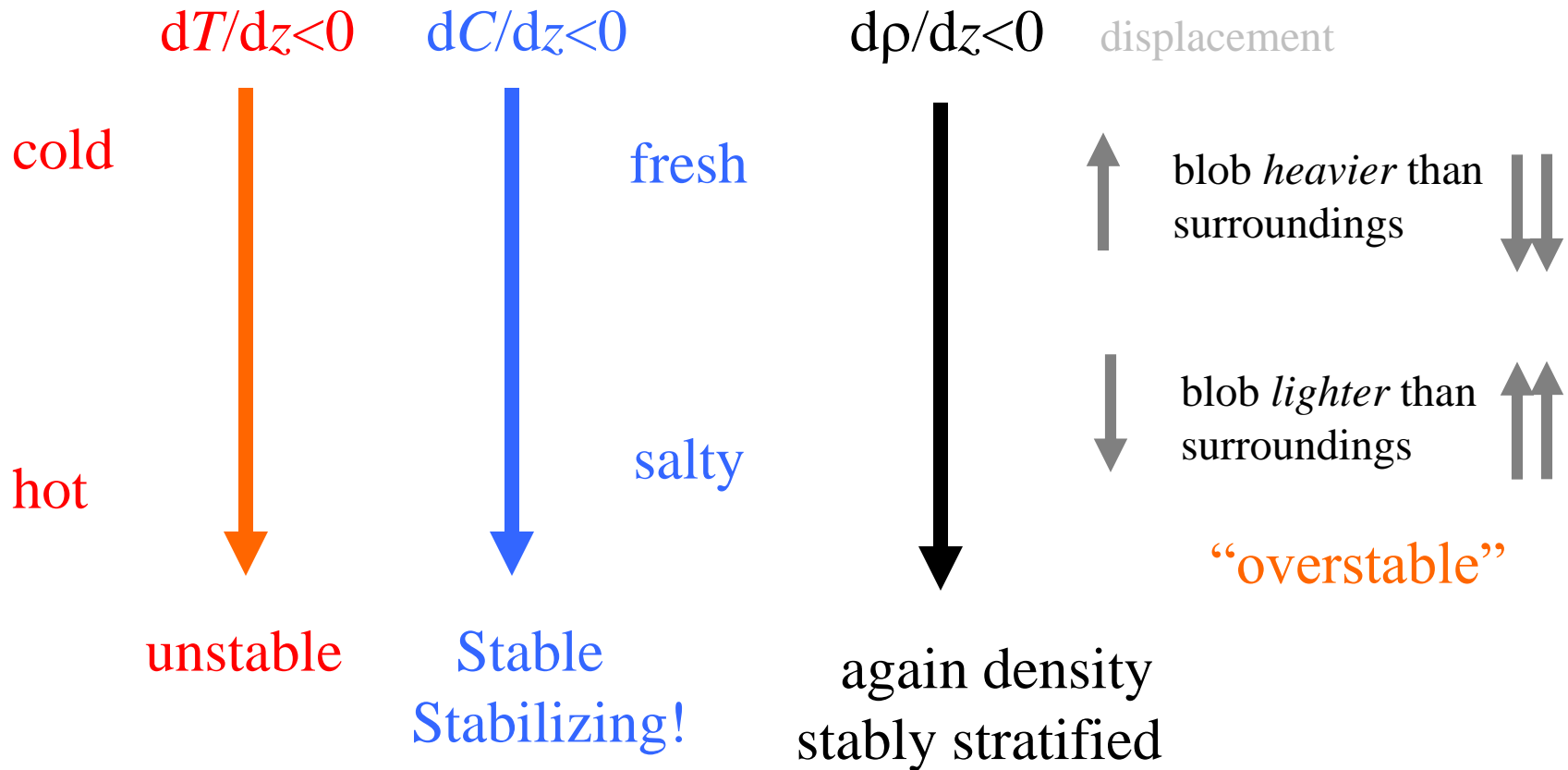
Origin in oceanography

- Stommel et al (1954) 
- Stern (1960)

Case 1: more salt on top



Case 2: salt stabilizes unstable dT/dz

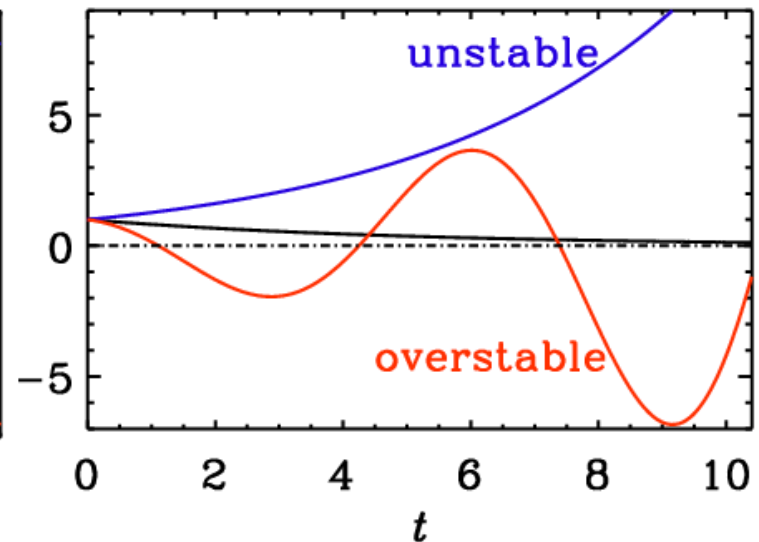
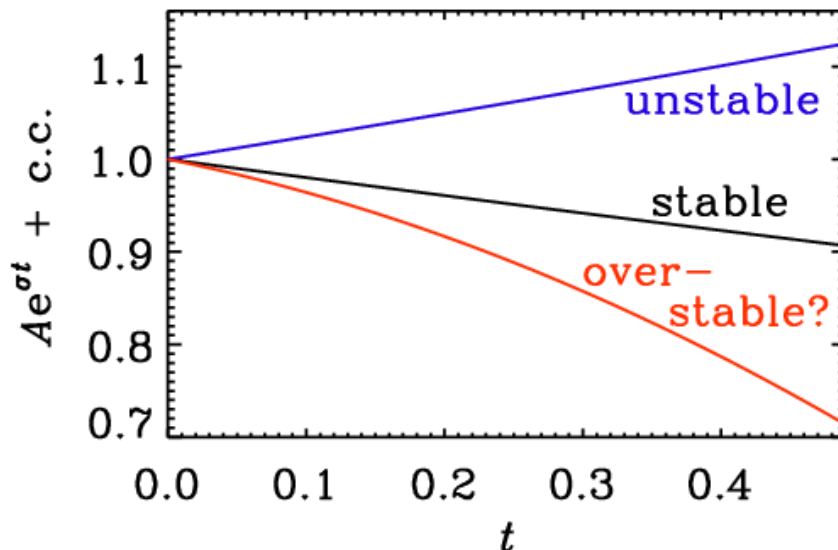


Overstability?

Originated from stellar stability →

ficient to keep up with the general diffusive loss from the core); these processes were estimated to dominate over the normal diffusive losses of an oscillation mode which tend to cool warm fluid and warm cool fluid, and therefore overall the heat engine does positive work to augment the kinetic and potential energies of the oscillation. **Eddington** dubbed such motion 'overstable'. Of course, in order to be sure that the nuclear driving is actually sufficient to dominate the diffusive damping in the Sun, a proper stability calculation had to be performed, but that (Christensen-

(Gough 2003)



→ Hopf bifurcation

Boussinesq equations

$$\frac{D\mathbf{u}}{Dt} = -\nabla \frac{P}{\rho_{00}} - \frac{\rho g}{\rho_{00}} + \nu \nabla^2 \mathbf{u}$$

($\rho_{00} = \text{const}$)

$$\frac{DT}{Dt} = \kappa_T \nabla^2 T$$

$$\frac{DC}{Dt} = \kappa_C \nabla^2 C$$

$$\rho = \rho_{00} [1 - \alpha_T (T - T_{00}) + \alpha_C (C - C_{00})]$$

Recall lecture 3, eq.(10) and (11)

linearized, &
double-curl

$$\left(\frac{\partial}{\partial t} - \nu \nabla^2 \right) u_{1z} = \alpha g \nabla_{\perp}^2 T_1$$

$$\left(\frac{\partial}{\partial t} - \kappa \nabla^2 \right) T_1 = \beta u_{1z}$$

Proceed analogously

$$\left(\frac{\partial}{\partial t} - \nu \nabla^2 \right) u_{1z} = \alpha_T g \nabla_{\perp}^2 T_1 - \alpha_C g \nabla_{\perp}^2 C_1$$

$$\left(\frac{\partial}{\partial t} - \kappa_T \nabla^2 \right) T_1 = \beta_T u_{1z}$$

$$\left(\frac{\partial}{\partial t} - \kappa_C \nabla^2 \right) C_1 = \beta_C u_{1z}$$

where

$$\beta_T = -\frac{dT_0}{dz}$$

$$\beta_C = -\frac{dC_0}{dz}$$

Reduce to single equation

apply $\left(\frac{\partial}{\partial t} - \kappa_T \nabla^2\right) \left(\frac{\partial}{\partial t} - \kappa_C \nabla^2\right)$

to both sides of

$$\left(\frac{\partial}{\partial t} - \nu \nabla^2\right) u_{1z} = \alpha_T g \nabla_{\perp}^2 T_1 - \alpha_C g \nabla_{\perp}^2 C_1$$

and use on rhs

$$\left(\frac{\partial}{\partial t} - \kappa_T \nabla^2\right) T_1 = \beta_T u_{1z}$$

$$\left(\frac{\partial}{\partial t} - \kappa_C \nabla^2\right) C_1 = \beta_C u_{1z}$$

....to obtain

$$\left(\frac{\partial}{\partial t} - \kappa_T \nabla^2\right) \left(\frac{\partial}{\partial t} - \kappa_C \nabla^2\right) \left(\frac{\partial}{\partial t} - \nu \nabla^2\right) \nabla^2 u_{1z} =$$
$$\left[\left(\frac{\partial}{\partial t} - \kappa_C \nabla^2\right) \alpha_T \beta_T - \left(\frac{\partial}{\partial t} - \kappa_T \nabla^2\right) \alpha_C \beta_C \right] g \nabla_{\perp}^2 u_{1z}$$

Do simplest case: stress-free boundaries

$$(\sigma + \kappa_T k^2)(\sigma + \kappa_C k^2)(\sigma + \nu k^2) k^2 = [(\sigma + \kappa_C k^2) \alpha_T \beta_T - (\sigma + \kappa_T k^2) \alpha_C \beta_C] g k_{\perp}^2$$

assume that principle of exchange of stabilities applicable

$$\kappa_T \kappa_C \nu k^6 = \kappa_C [\alpha_T \beta_T - \kappa_T \alpha_C \beta_C] g k_{\perp}^2$$

...works only for nonoscillatory onset

But we see that that instability is possible if

$$\frac{k^6}{k_{\perp}^2} = \frac{\alpha_T \beta_T g}{\nu \kappa_T} - \frac{\alpha_C \beta_C g}{\nu \kappa_C}$$

remember:

$$\beta_T = -\frac{dT_0}{dz}$$
$$\beta_C = -\frac{dC_0}{dz}$$

Either negative T gradient big enough (i.e. 1st term dominant):

→ similar to Rayleigh-Benard convection

but could be stabilized by negative C gradient

or C gradient is positive and big enough (2nd term dominant):

→ salt fingers

Dispersion relation

substitute

$$\sigma \rightarrow \underbrace{\sigma / \nu k^2}_{\equiv \sigma_\nu}$$

Buoyancy
frequencies

$$N_T^2 = \alpha_T \beta_T g$$

$$N_C^2 = \alpha_C \beta_C g$$

→ Cubic equation

$$\sigma^3 + \sigma^2(\kappa_T + \kappa_C + 1) + \sigma[\kappa_T \kappa_C + \kappa_C + \kappa_T + (N_T^2 - N_C^2)k_\perp^2] + \kappa_T \kappa_C + (N_T^2 \kappa_C - N_C^2 \kappa_T)k_\perp^2 = 0$$

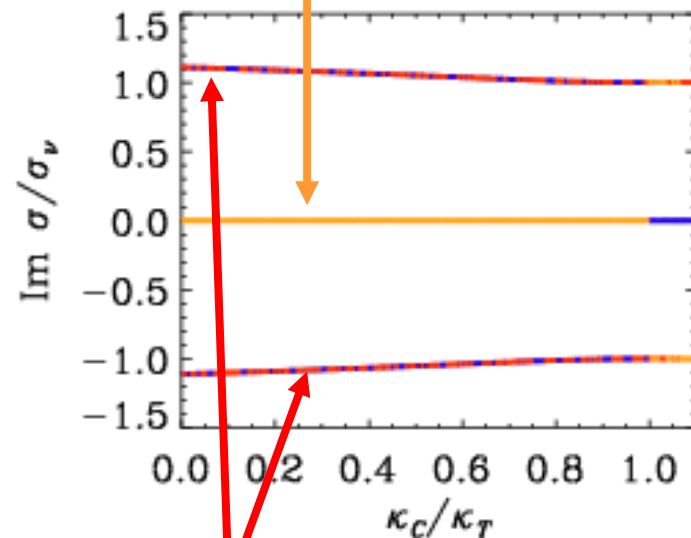
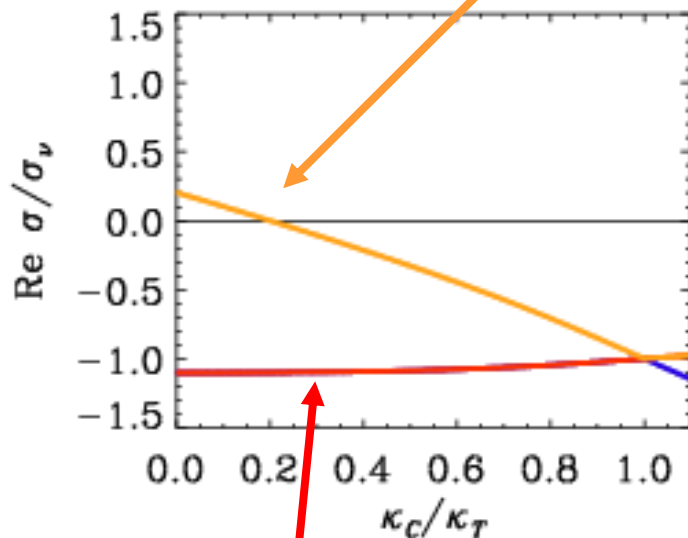
Solve numerically

Onset, nonoscillatory (zero frequency)

$$N_T^2 = -3$$

$$N_C^2 = -1$$

$$k_\perp^2 = 0.5$$



also: decaying, oscillatory modes (pair of finite frequencies)

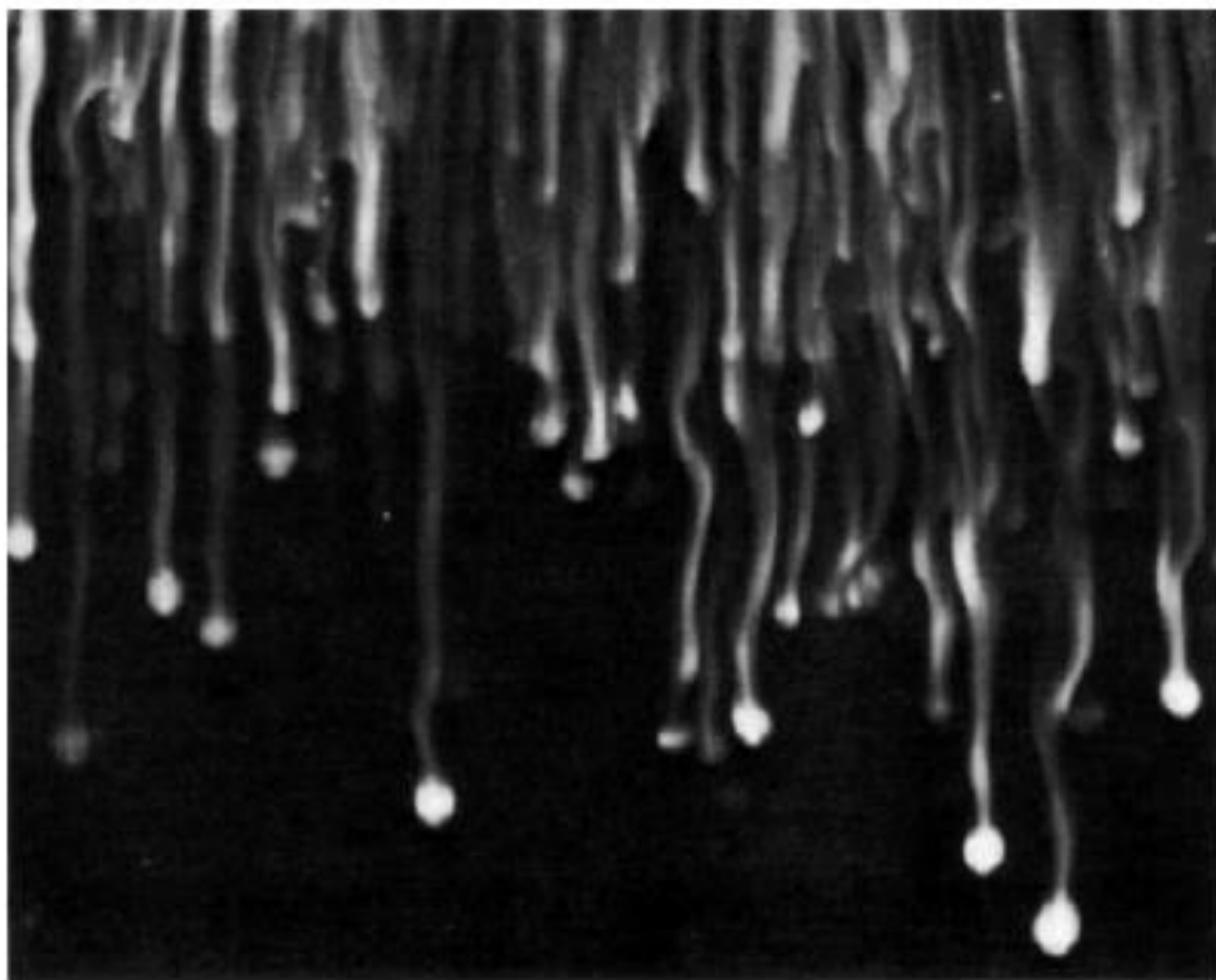
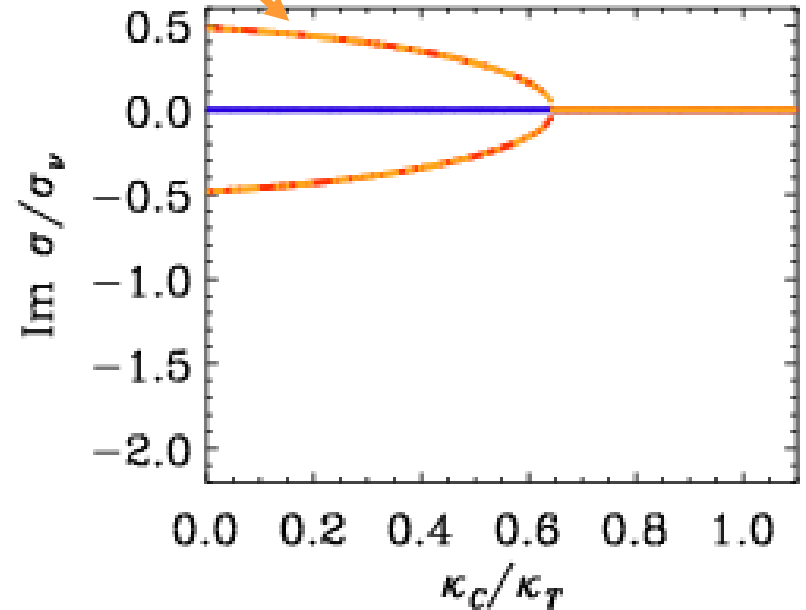
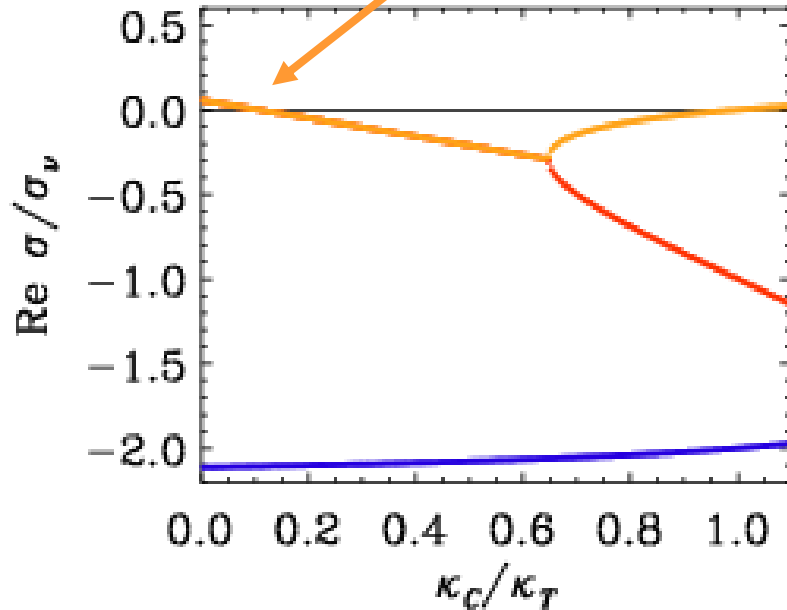


Figure 12.8 Salt fingers, produced by pouring salt solution on top of a stable temperature gradient. Flow visualization by fluorescent dye and a horizontal beam of light. J. Turner, *Naturwissenschaften* **72**: 70–75, 1985 and reprinted with the permission of Springer-Verlag GmbH & Co.

Dispersion relation: opposite case

growing oscillatory modes
(again pair of frequencies)

$$N_T^2 = +3$$
$$N_C^2 = +1$$
$$k_{\perp}^2 = 0.5$$



The two regimes

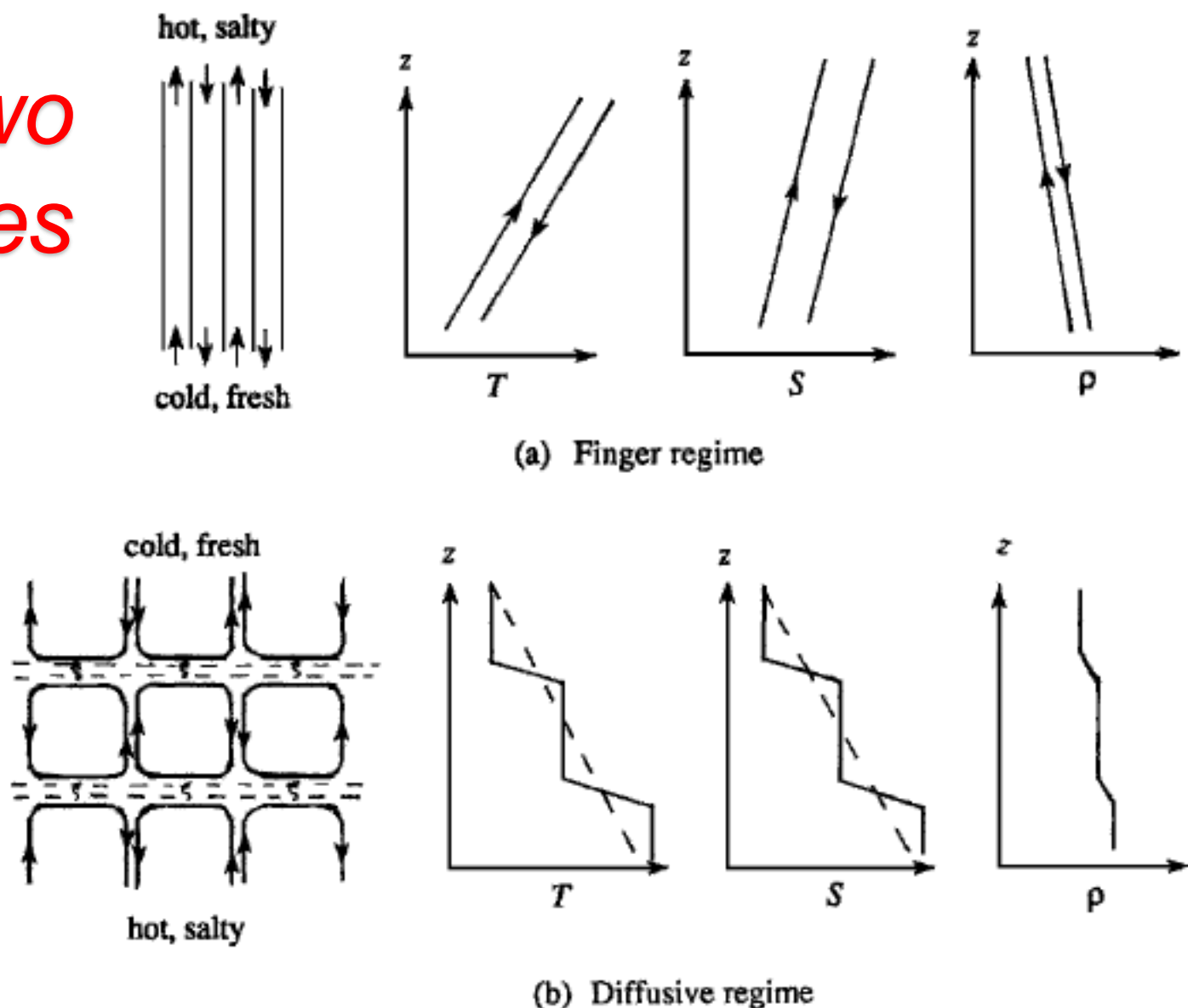


Figure 12.7 Two kinds of double-diffusive instabilities. (a) Finger instability, showing up- and downgoing salt fingers and their temperature, salinity, and density. Arrows indicate direction of motion. (b) Oscillating instability, finally resulting in a series of convecting layers separated by "diffusive" interfaces. Across these interfaces T and S vary sharply, but heat is transported much faster than salt.

Staircase formation

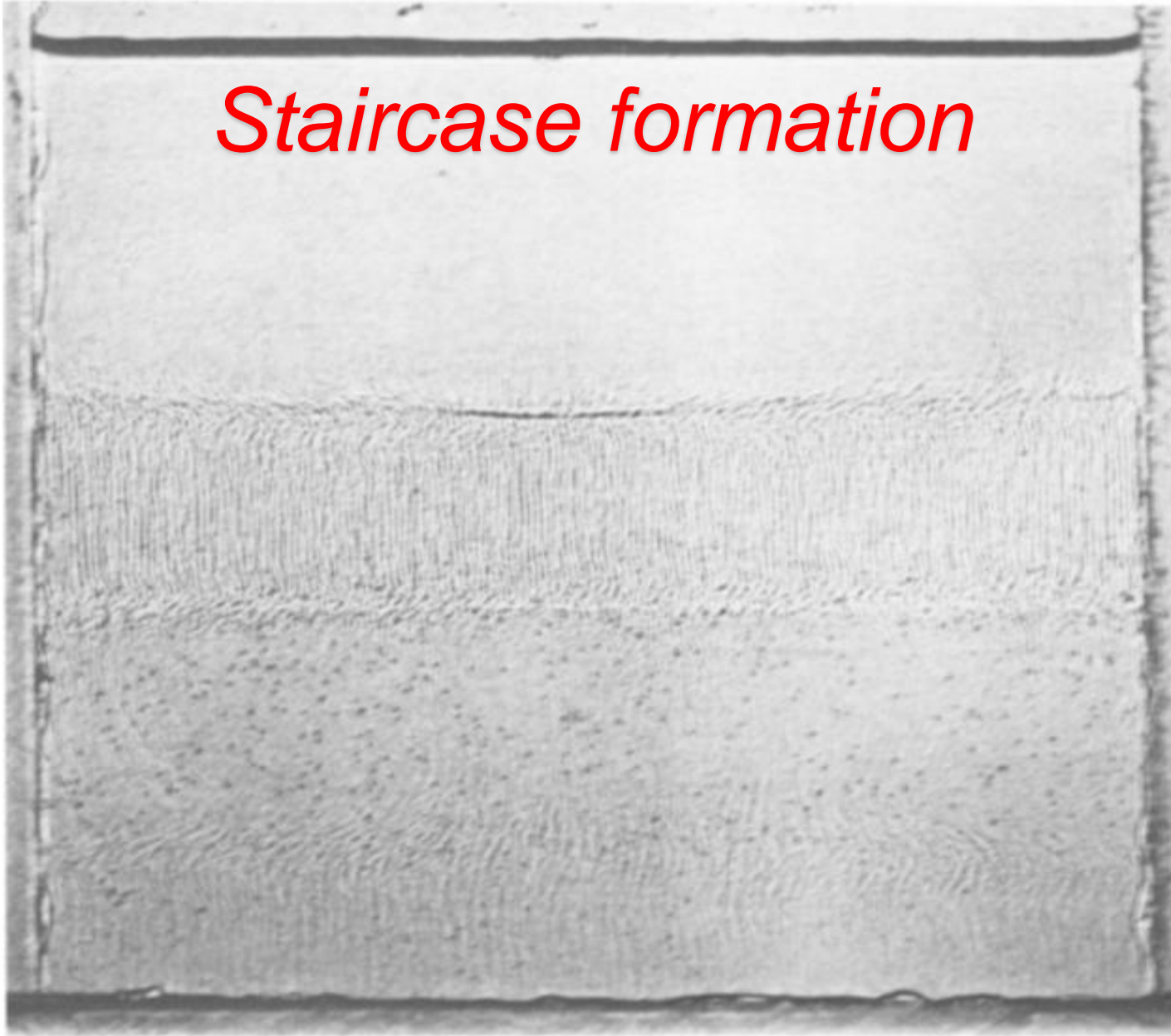


Fig. 4. Shadowgraph of a “finger” interface, formed between an aqueous solution of sugar (the more slowly diffusion solute) above a denser layer of NaCl solution.

Staircase formation

Empirical fact, not from linear theory (nor weakly nonlinear theory)

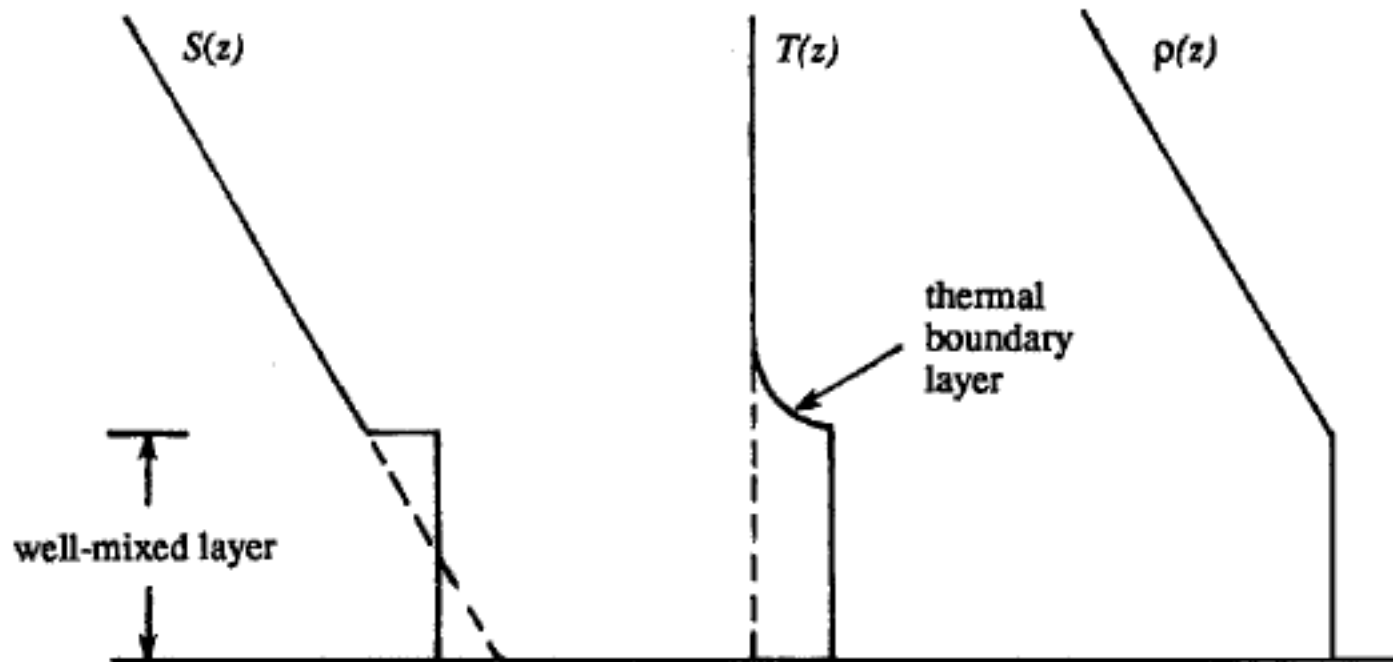
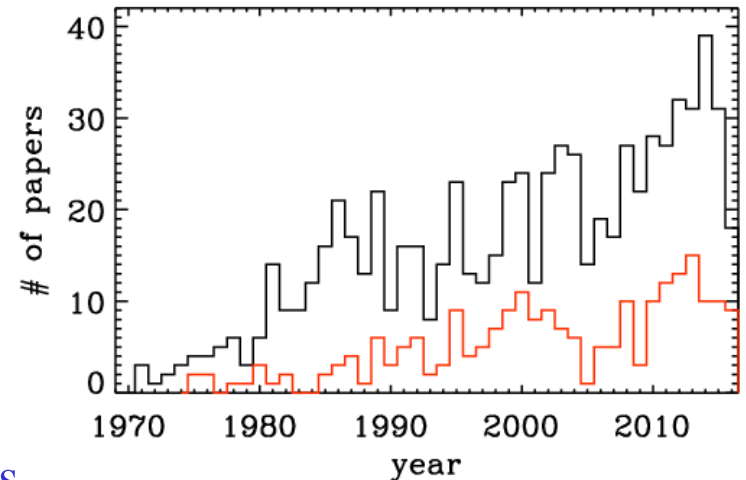


Figure 12.9 Distributions of salinity, temperature, and density, generated by heating a linear salinity gradient from below.

Many applications!

- Oceanography
- Geology (magma chambers)
- Astrophysics
- Engineering (metallurgy)

Publications in double-diffusive



Yet, not very highly thought of back in the 1950s

It seems premature to speculate upon the improbable practical importance of this phenomenon for pumping up nutrient rich deep water to the surface for fish-farming applications, or its inverse for removing waste products to the deep water. As a power source it is quite unpromising. Thus it remains essentially a curiosity.

HENRY STOMMEL
ARNOLD B. ARONS
DUNCAN BLANCHARD

Contribution No. 799 of The Woods Hole Oceanographic Institution, Woods Hole, Mass., U.S.A.

Astrophysical application: μ -gradient

Kato (1966)

Note added on September 20, 1966: Since this paper was submitted for publication, the author received some important comments from Dr. Edward A. Spiegel. Spiegel pointed out that the existence of overstable convection has already known in the salt convection problem by G. VERONIS (*J. Marine Research* 23, 1, 1965; see also STERN, *Tellus*, 12, 172, 1960). The present problem is formally identical to the salt problem apart from some subtleties of radiation.

vection) may occur if the medium is thermally conductive. This possibility of growing oscillatory convection was predicted by CHANDRASEKHAR (1) and was explained physically by COWLING ((2), see also LEDOUX (3)). Heat exchange leads to asymmetries in the oscillatory motion in such a way that an oscillating fluid element returns with a higher velocity than it had when it left the exuililibrium position and the oscillation is amplified in each cycle. MOORE and and SPIEGEL (4)

STELLAR MODELS WITH CONVECTION AND WITH DISCONTINUITY
OF THE MEAN MOLECULAR WEIGHT

P. LEDOUX

Yerkes Observatory

Received December 9, 1946

In astrophysics: semi-convection

ON THE OCCURRENCE OF SEMI-CONVECTION IN MASSIVE STARS

R. J. Tayler

(Received 1968 December 2)

Overstable Convection in a Medium Stratified in Mean Molecular Weight

Shoji KATO

Department of Astronomy, University of Tokyo, Tokyo

(Received September 5, 1966)

Abstract

In the medium stratified in mean molecular weight the condition for on convection is known as

$$\nabla \geq \nabla_{ad} + \frac{\beta}{4-3\beta} \frac{d \ln \mu}{d \ln p}$$

The properties of g-modes in layered semiconvection

Mikhail A. Belyaev,¹★ Eliot Quataert¹ and Jim Fuller^{2,3}

¹Astronomy Department and Theoretical Astrophysics Center, University of California Berkeley, Berkeley, CA 94720, US.

²TAPIR, Walter Burke Institute for Theoretical Physics, Mailcode 350-17, California Institute of Technology, Pasadena, CA 91125, USA

³Kavli Institute for Theoretical Physics, Kohn Hall, University of California, Santa Barbara, CA 93106, USA

Accepted 2015 June 26. Received 2015 June 26; in original form 2015 May 20

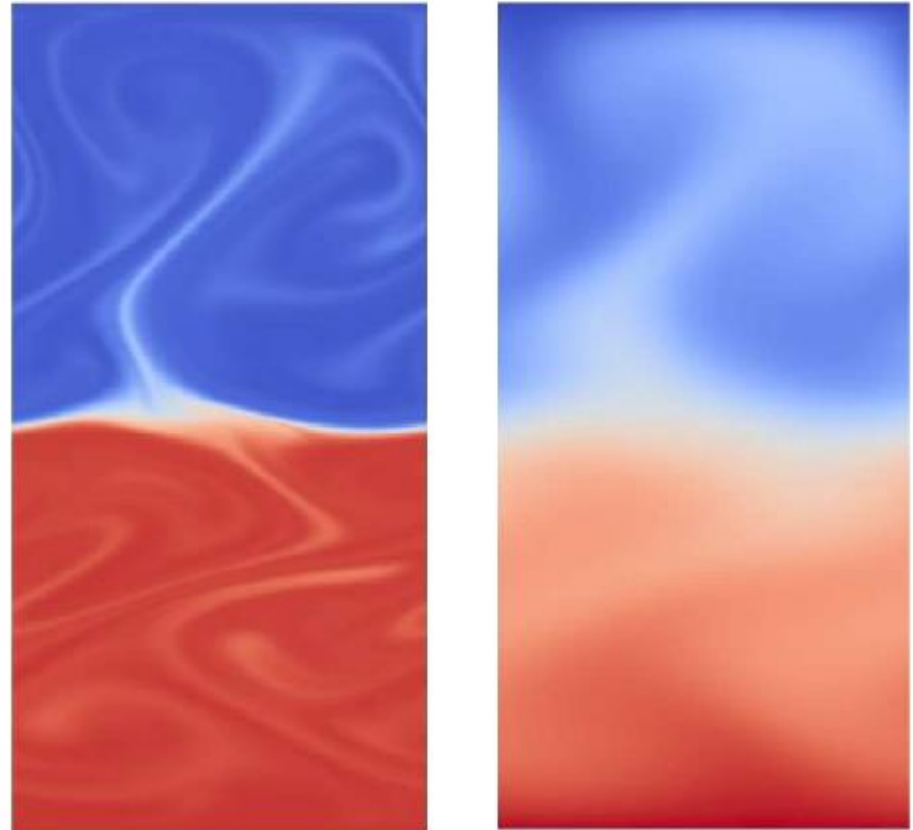


Fig. 7. Snapshot of a simulation including the free interface between two layers. *Left:* solute, *Right:* temperature. $Pr = 1.0$, $Le = 0.01$, $R_\rho = 1.15$, $Ra_* = 6 \times 10^5$. See also the movie online.

→ Lots of current research!

Layered convection
(Zaussinger & Spruit 2013)

Backup slides

Transitions to chaos in two-dimensional double-diffusive convection

By EDGAR KNOBLOCH

Department of Physics, University of California, Berkeley, CA 94720, USA

DANIEL R. MOORE

Department of Mathematics, Imperial College, London SW7 2BZ, UK

JURI TOOMRE

Joint Institute for Laboratory Astrophysics and Department of Astrophysical, Planetary and
Atmosphere Sciences, University of Colorado, Boulder, CO 80309, USA

AND NIGEL O. WEISS

Department of Applied Mathematics and Theoretical Physics, University of Cambridge,
Cambridge CB3 9EW, UK

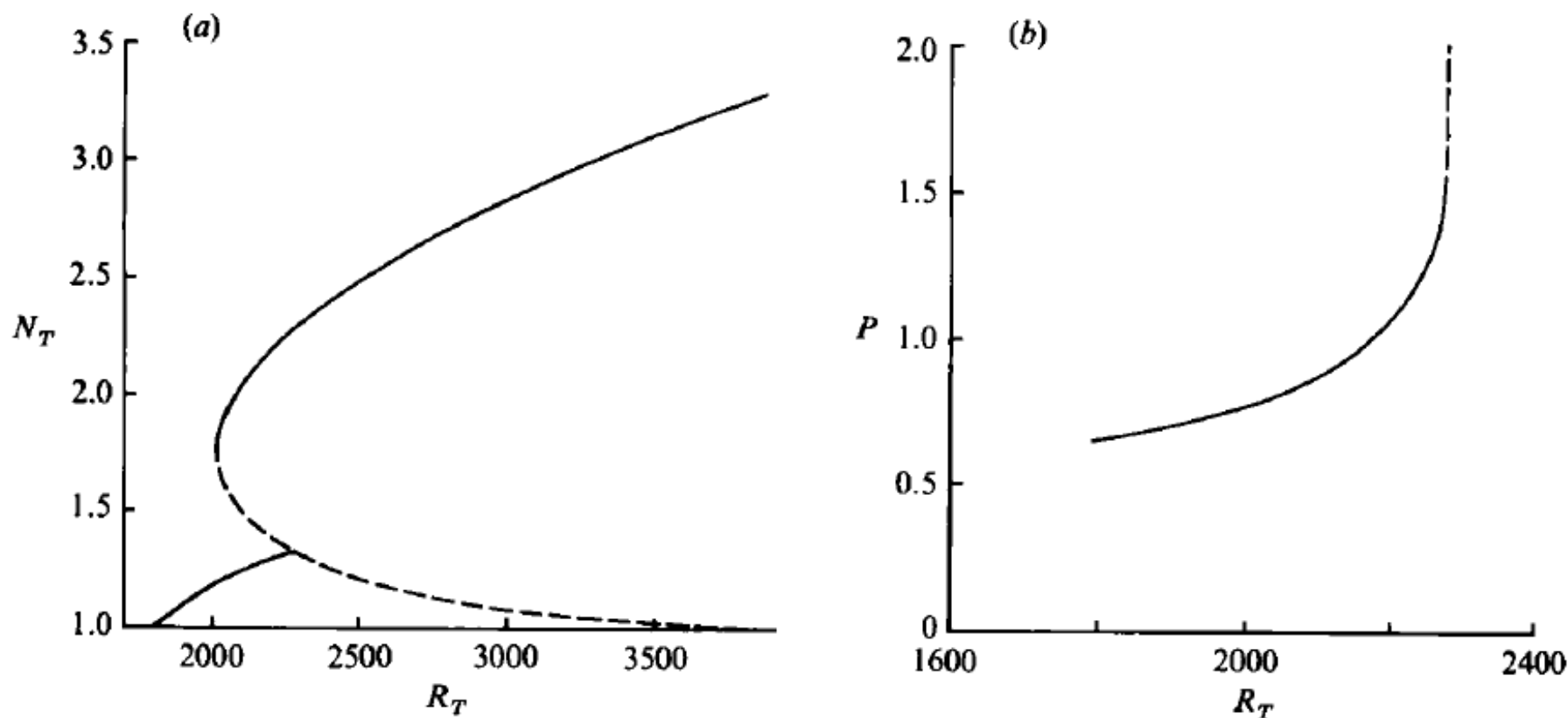


FIGURE 2. (a) Numerical Nusselt number–Rayleigh number (N_T – R_T) diagram for the partial differential equations with $\lambda = 1.414$, $\sigma = 1.0$, $\tau = 0.316$ and $R_S = 10^3$ showing that the branch of oscillatory solutions still terminates on the branch of unstable steady solutions at $R_T^{(c)} \simeq 2280$. (b) The period P of the oscillations as R_T approaches $R_T^{(c)}$. The sharp rise in the period is characteristic of the approach to the heteroclinic limit cycle (after Huppert & Moore 1976).

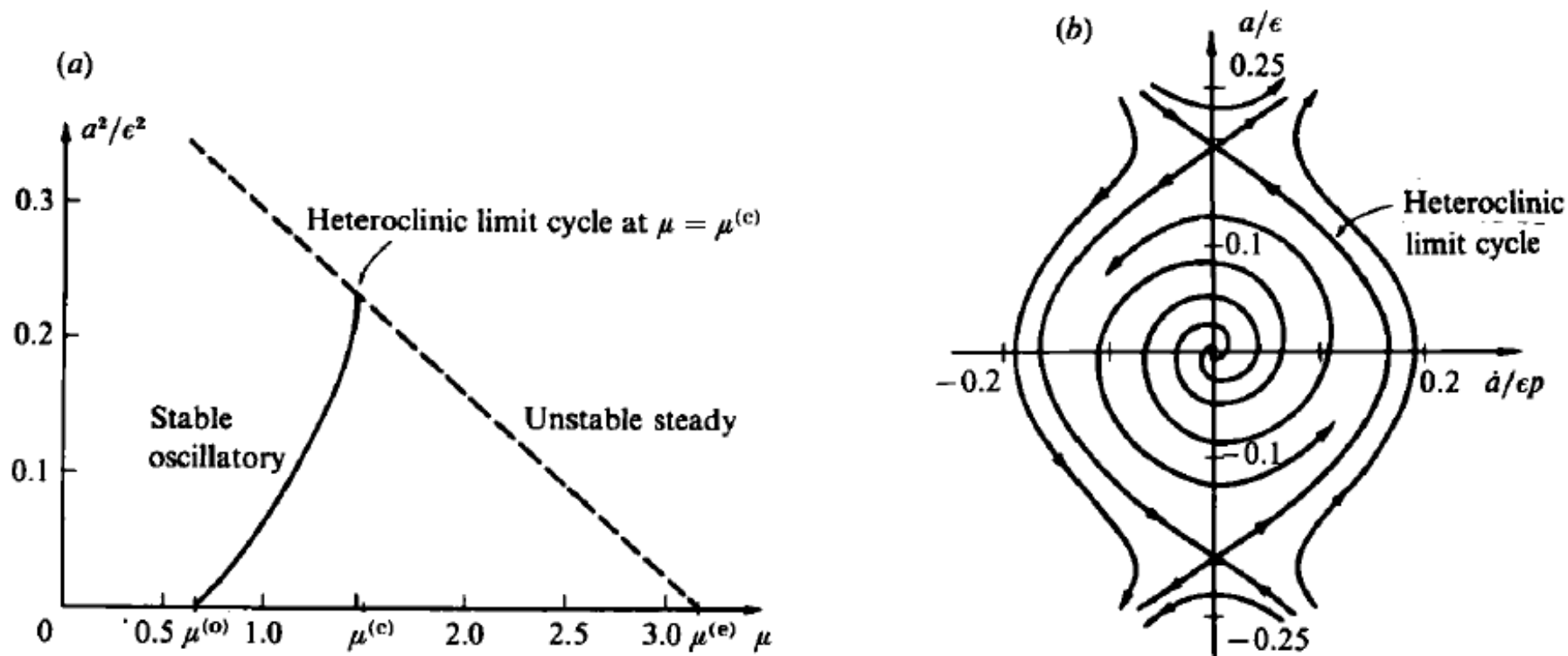


FIGURE 1. (a) Analytical amplitude-Rayleigh number ($a-r_T$) diagram for the partial differential equations with $\sigma = 1.0$, $\tau = 0.316$ and $r_S = r_S^{(c)} + \epsilon^2$, $\epsilon \ll 1$, showing that the branch of oscillatory solutions (solid line) terminates on the branch of unstable steady solutions (broken line) at $\mu = \mu^{(c)} \simeq 1.468$, where $\mu = (r_T - 1.925)/\epsilon^2$. (b) Phase portrait at $r_T = r_T^{(c)}$ showing a heteroclinic limit cycle joining two saddle points (after Knobloch & Proctor 1981).

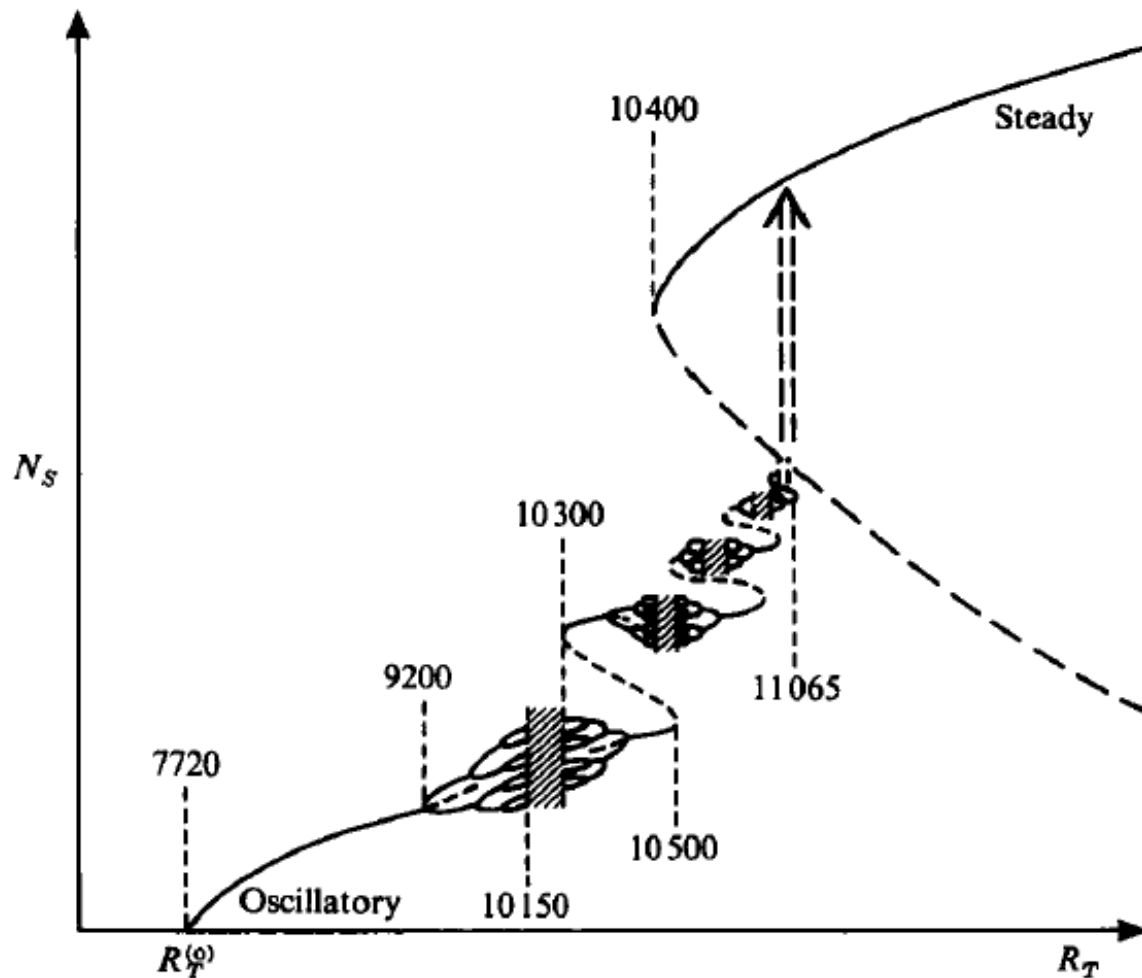


FIGURE 6. Steady and oscillatory solutions of the partial differential equations: schematic bifurcation diagram of the solutal Nusselt number N_S as a function of R_T . Note the bubbles of period-doubling bifurcations on the first and second oscillatory branches, the hysteresis loop connecting the two branches and subsequent (conjectured) branches. Conjectured unstable solutions are indicated by broken lines.

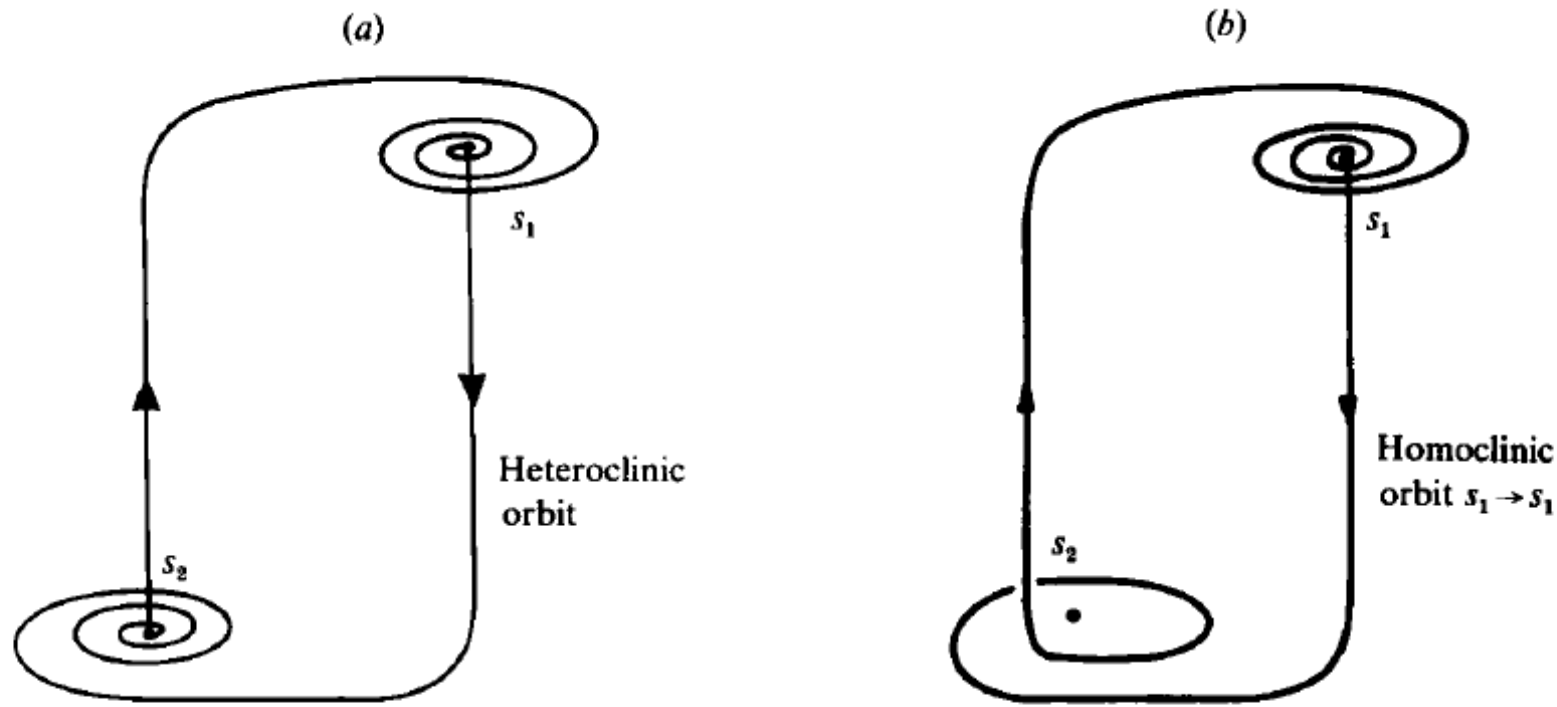


FIGURE 4. The fifth-order model: (a) Sketch of a heteroclinic limit cycle connecting saddle-foci; (b) Sketch of a possible homoclinic limit cycle.

“Salt fingers” in magma chamber

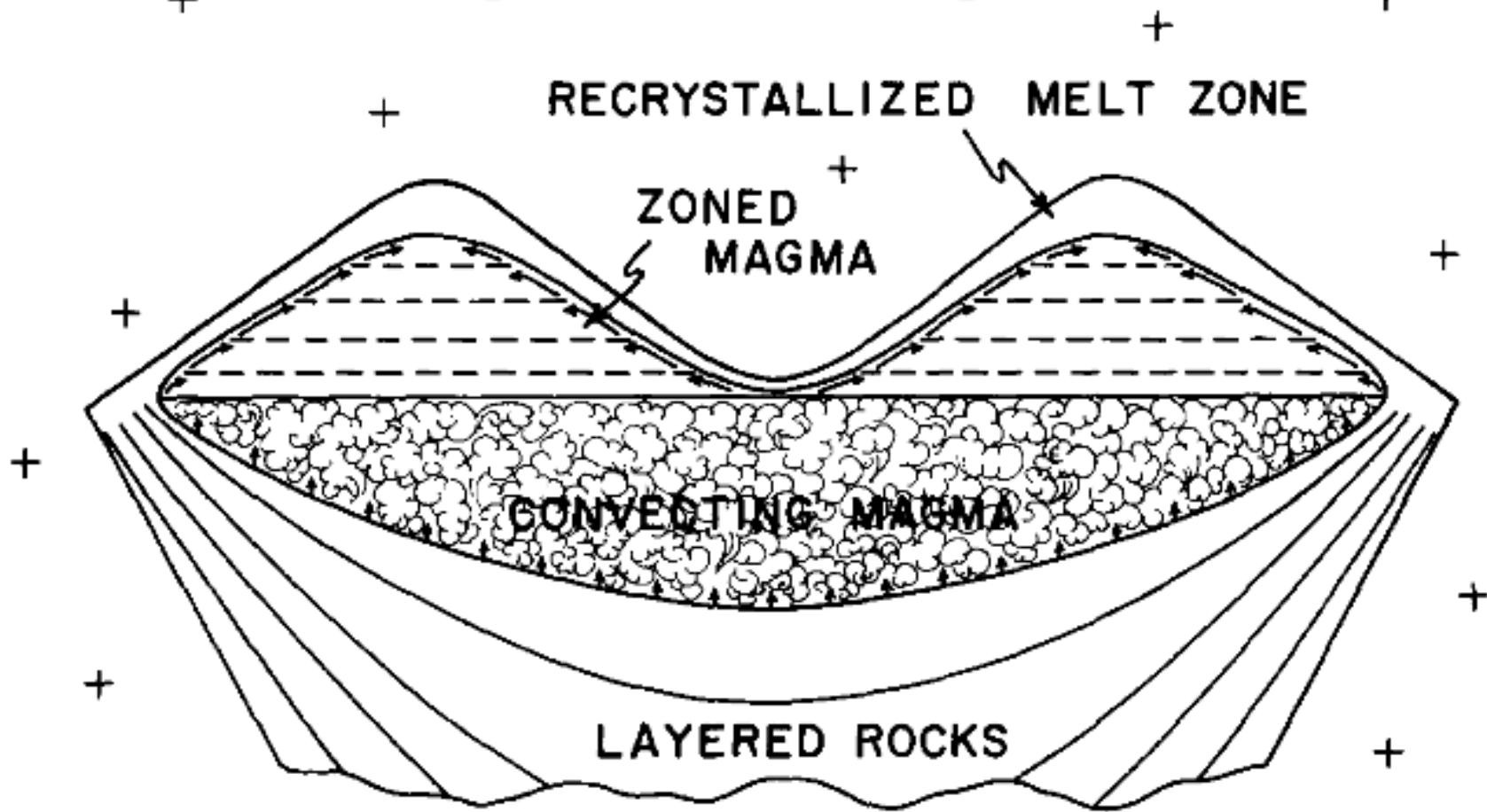
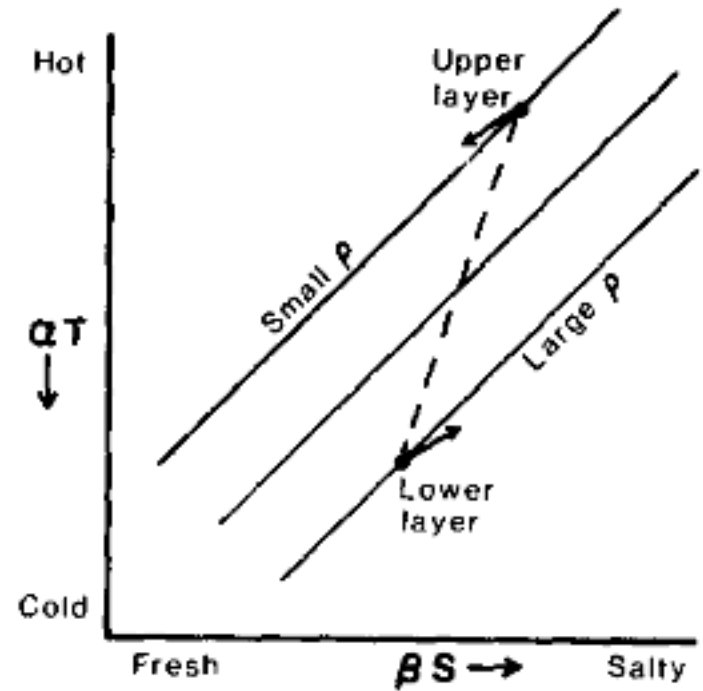
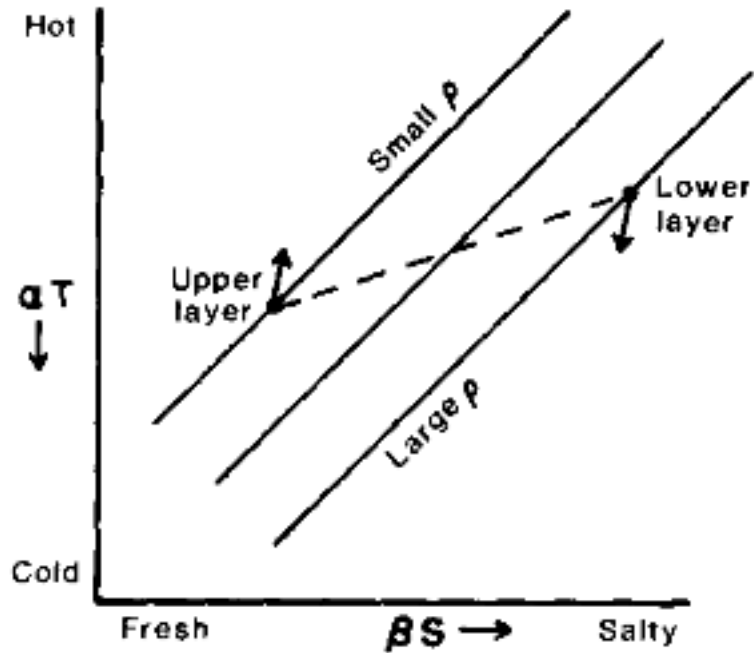


Fig. 27. Diagrammatic representation of convection in a magma chamber which has melted its roof, after the melt layer has begun to crystallize. Note that the vertical scale is exaggerated and that only the top of the chamber is shown.

Comparison: the 2 regimes



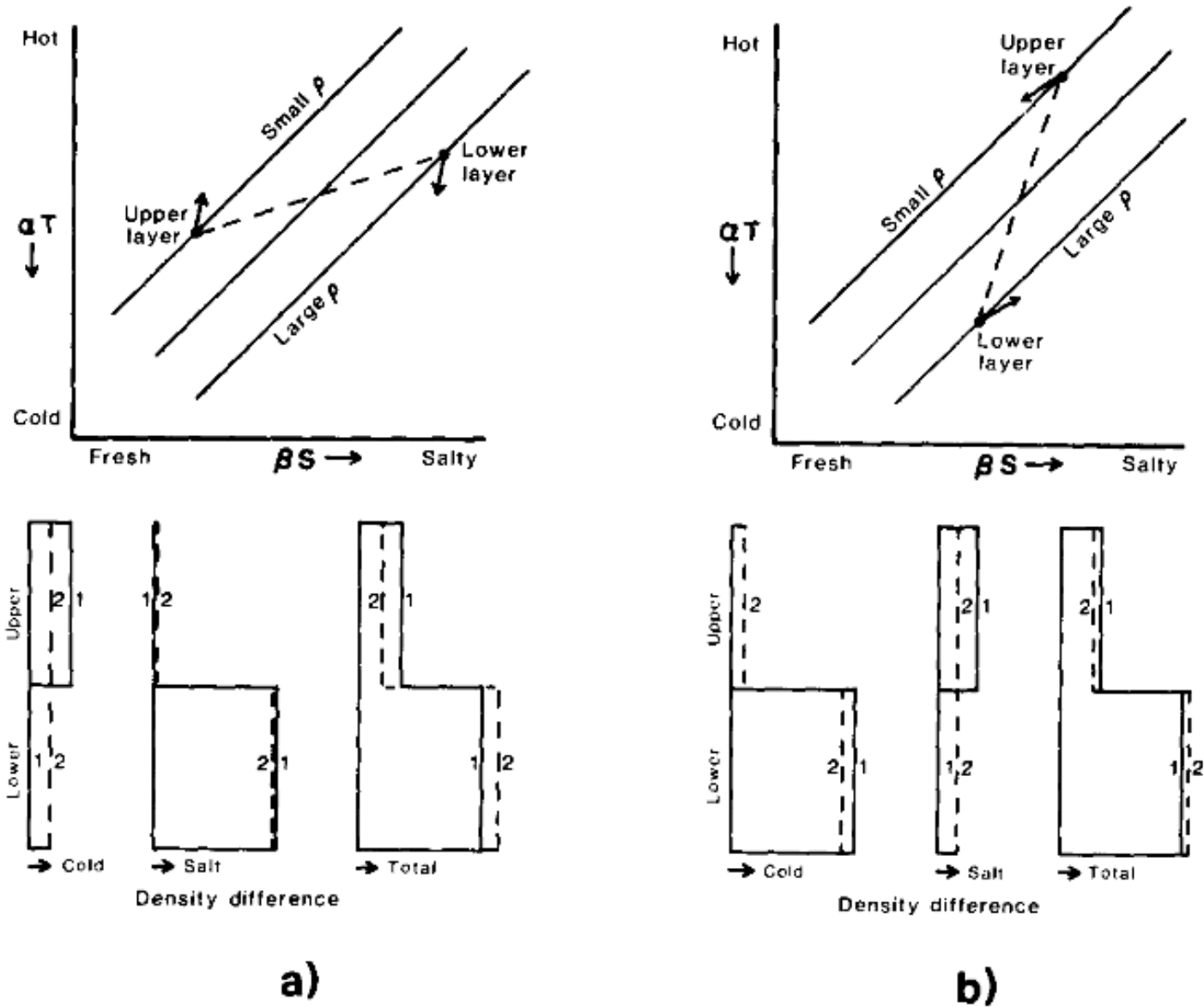


Fig. 5. Showing the changes in T , S and ρ in layers separated by (a) a diffusive and (b) a finger interface due to the double-diffusive fluxes across the interface. In each case the originally unstably distributed component (the driving component) is transported more rapidly, until it "runs down" and becomes uniformly distributed in the vertical. The net density difference between the layers always increases during both processes.